J. Fluid Mech. (1995), *vol.* 292, *pp.* 229–248
Copyright © 1995 Cambridge University Press

On penetrative convection at low Péclet number

By JOHN R. LISTER

Institute of Theoretical Geophysics, Department of Applied Mathematics and Theoretical Physics, University of Cambridge, Silver Street, Cambridge CB3 9EW, UK

(Received 4 March 1994 and in revised form 4 January 1995)

A new theoretical model is developed for the growth of a convecting fluid layer at the base of a stable, thermally stratified layer when heated from below. The imposed convective heat flux is taken to be comparable to the heat flux conducted down the background gradient so that diffusion ahead of the interface between the convecting and stable layers makes a significant contribution to the interfacial heat flux and to the rate of rise of the interface. Closure of the diffusion problem in the stable region requires the interfacial heat flux to be specified, and it is argued that this is determined by the ability of convective eddies to mix warmed fluid below the interface downwards. The interfacial velocity, which may be positive or negative, is then determined by the joint requirements of continuity of heat flux and temperature. A similarity solution is derived for the case of an initially linear temperature gradient and uniform heating. Solutions are also given for a heat flux that undergoes a step change and for a heat flux determined from a four-thirds power law with a fixed base temperature. Numerical calculations show that the predictions of the model are in good agreement with previously reported experimental measurements. Similar calculations are applicable to a wide range of geophysical problems in which the tendency for diffusive restratification is comparable to that for mixed-layer deepening by entrainment.

1. Introduction

There are many geophysical situations in which a turbulent fluid layer is separated from a stably stratified layer by a relatively sharp interface. Examples include the oceanic upper mixed layer and underlying pycnocline, the atmospheric convective layer and overlying stratosphere, the convection and radiation zones in stars (Schwarzschild 1958), lakes undergoing penetrative convection (Carmack & Farmer 1982), turbidity currents in stably stratified environments (Kerr 1991), and convecting and conducting zones in magma chambers (Jaupart & Brandeis 1986) and possibly in the Earth's core (Gubbins, Thomson & Whaler 1982). Environmental applications include mixing in solar ponds, dispersal of buoyant pollutants and reservoir management. In each case the quantities of most interest are the rate of buoyancy transfer across the interface between the layers and the rate of migration of the interface.

Studies of entrainment across interfaces have drawn distinctions between mixing due to turbulent flows with zero and with non-zero mean shear, and between flow generated by convective motions and by mechanical mixing. References to the extensive literature in the field can be found in the monographs by Turner (1973) and Zilitinkevich (1991) and in the review by Fernando (1991). Many of the investigations of zero-mean-shear mixing have used the mixing-box configuration of Rouse & Dodu (1955) in which the turbulence is generated by an oscillating rectangular grid. Debate has centred on the energetics of the turbulent flow, on the mechanisms of mixing such

as 'splashing' by impinging eddies (Linden 1973), interfacial wave breaking (Fernando & Long 1985; Hannoun & List 1988) and Kelvin–Helmholtz instabilities (Hannoun & List 1988; Mory 1991), on whether the asymptotic dependence of the entrainment rate at large Richardson number Ri is proportional to Ri^{-1}, $Ri^{-3/2}$ or $Ri^{-7/4}$ and on the thickness of the interfacial layer.

A significant feature of all this work is that the Péclet number is assumed to be sufficiently large that molecular diffusion of the stratifying component (heat, salt, etc.) can be neglected in the bulk of the stratified region. As a result, the buoyancy flux across the interface is primarily advective, rather than diffusive, and caused by turbulent erosion of the stratified region. In this paper we consider the opposite limit of low Péclet number in which the diffusive flux from a strongly stratified region is the dominant contribution to the buoyancy flux across the interface. It may be noted that there is in general a competition between the tendency of diffusion to stabilize the turbulent region and the tendency of the turbulence to erode the stratified region. At high Péclet number the turbulent region inevitably grows at the expense of the stratified region. At low Péclet number the competition is more evenly matched and the interface between the stratified and turbulent regions may be held stationary or even advance at the expense of the turbulent region. It is this situation we propose to model.

Comparatively little is known about low-Péclet-number entrainment despite its relevance to diffusive restratification. An indication of the significance of the Péclet number Pe is given by a comparison of the experimental results of Fernando & Little (1990), which show that there is little or no effect of diffusion on the entrainment rate when $Pe > 10^3$, and those of Crapper & Linden (1974), which show that the interfacial thickness between two grid-stirred turbulent layers is diffusively controlled when $Pe < 200$. Various authors (e.g. Phillips 1977; Hannoun & List 1988; Noh & Fernando 1993) have suggested that entrainment is diffusively controlled, and therefore dependent on the Péclet number, when the Richardson number is sufficiently large that wave breaking is suppressed in the interfacial zone between grid-stirred and stratified regions. These studies are at sufficiently large Péclet number that diffusion influences only the interfacial zone and do not address the case considered here in which diffusion influences the bulk of the stratified layer. Hopfinger & Linden (1982) experimentally investigated the competition between stratification and turbulent entrainment in a fluid heated from above and stirred by a grid from below. At low rates of surface heating the turbulence kept the fluid column well-mixed; at larger rates of heating a steady stable surface layer was formed through which the conductive heat flux balanced the underlying turbulent flux; and at still larger rates of heating the surface stratification increased continually. An important feature of their explanation of the results is the decay of the turbulence with vertical distance above the grid. This spatial decay is a significant difference between the structure of grid-stirred turbulence and that driven by convection.

The study most closely related to the present paper is that of Denton & Wood (1981, referred to hereafter as DW), who presented experimental results and a model for the erosion of a stable temperature gradient by heating from below at low Péclet number. Following a discussion in §2 of the mechanism of interfacial motion when diffusion is dominant, we propose a new, physically motivated boundary condition that closes the diffusion problem in the stable region and determines the interfacial motion. This boundary condition was not present in the model of DW, who closed the problem, possibly unconsciously, by the way they solved their equations numerically. In §3 we derive a similarity solution to the governing equations with the new boundary condition for the case of an initially linear temperature profile heated steadily from below.

Solutions for a heat flux that undergoes a step decrease and for a heat flux determined from a four-thirds power law with a fixed base temperature show how the convecting region can be restratified if the heat is not maintained. The experimental data of DW are reanalysed in §4 using the new boundary condition and very good agreement is obtained. Further discussion is given in §5.

It should be noted that, in the present problem, the Péclet number may be defined as the ratio of the advective heat flux in the convecting region either to the small conductive flux in the convecting region or to the much larger background conductive flux in the stably stratified region. This distinction has not been clearly drawn in the preceding literature. In order to reduce possible ambiguity but still retain links with existing terminology, we use the terms convective Péclet number or *Pe* to refer to the former definition, but the terms high and low Péclet number or global Péclet number to refer to the latter definition. Formulae are given in Appendix A.

2. The model and equations

We consider a thermally stratified fluid being heated uniformly from its lower boundary. Based on experimental observations (e.g. Deardorff, Willis & Lilly 1969; Deardorff, Willis & Stockton 1980; DW), we divide the fluid conceptually into four regions (figure 1*a*). At large distances above the heated lower boundary the fluid is essentially stagnant and heat transfer is by diffusion alone. Between the diffusive region and the boundary lies a (growing) thermally convecting region in which the fluid is well-mixed and the heat transfer is predominantly by turbulent advection. (Viscously dominated convection in a high-Prandtl-number fluid is considered briefly in Appendix B.) The third region is the thermal boundary layer between the well-mixed convecting region and the heated boundary. This layer is heated diffusively by the adjacent boundary, becomes buoyant and unstable, and intermittently detaches from the boundary to rise as a thermal into the overlying mixed layer (Lick 1965; Howard 1966). Provided the Rayleigh number based on the heat flux and the height of the convecting region is sufficiently large, the thickness of the basal boundary layer and the temperature anomalies within it can be neglected. Finally, there is an interfacial zone between the well-mixed region and the diffusive region in which rising thermals penetrate a short distance into the overlying stable stratification and are then returned to their level of neutral buoyancy. At low Péclet number this zone is much thinner than the vertical scale of the temperature variations in the overlying diffusive region and may also be neglected (see Appendix A; cf. also the small penetration distance into the diffusive core in the experiments at low Péclet number of Crapper & Linden 1974).

We are thus led to a simple two-layer model (figure 1*b*) in which the internal details of the basal thermal boundary layer and of the interfacial zone are represented only by their ability to transmit a heat flux between the boundary and the well-mixed region and between the well-mixed region and the diffusive region. Since the thickness of the interfacial zone is negligible, both the temperature and the heat flux are continuous across it. This model is similar to that used in previous analyses of low-Péclet-number penetrative convection (DW; Gubbins *et al.* 1982; Jaupart & Brandeis 1986), but our analysis differs in the equations and boundary conditions used to describe the layers. It should also be noted that the continuity conditions used at the interface differ from previous models of high-Péclet-number entrainment that include a temperature step at the interface between the well-mixed region and the stably stratified region. This is a reflection of the fact that a temperature discontinuity cannot be maintained when the diffusive heat flux above the interface plays a significant role, as considered here.

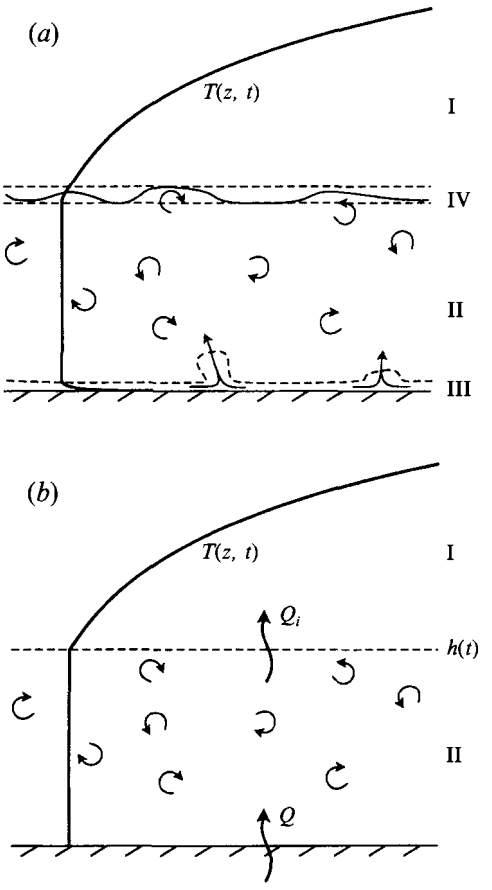

FIGURE 1. (*a*) Schematic representation of a stratified fluid being heated at its lower boundary. I, Stably stratified region in which heat transfer is by diffusion; II, well-mixed convecting region; III, basal thermal boundary layer, which intermittently ejects buoyant thermals; IV, interfacial zone given by the penetration distance of rising thermals. (*b*) The simplified two-layer model, which is the subject of the present analysis. A stable diffusive region I is separated from a well-mixed region II by an interface at height $z = h(t)$. The basal heat flux is Q and the interfacial heat flux Q_i.

Let the well-mixed region occupy $0 < z < h(t)$ and the stably stratified region $h(t) < z < \infty$. The temperature in the stably stratified region obeys the diffusion equation

$$\frac{\partial T}{\partial t} = \frac{\partial}{\partial z}\left(\kappa \frac{\partial T}{\partial z}\right). \tag{1}$$

An *ad hoc* representation of enhanced diffusion due to internal wave motion might be obtained by increasing the thermal diffusivity κ near the interface. In the following, however, we shall take κ to be the constant molecular value of diffusivity, both for simplicity to avoid using an empirical parameterization of wave-induced diffusion and because the experiments of DW showed that the interfacial heat flux was predominantly due to molecular diffusion (see §4). Equation (1) must be solved subject to the boundary conditions

$$T \to T_0 \quad \text{as} \quad z \to \infty, \tag{2a}$$

$$T \to T_0 \quad \text{as} \quad t \to 0, \tag{2b}$$

where $T_0(z)$ is the stable temperature profile at time $t = 0$ when the heating commences.

Let the imposed heat flux at the lower boundary be $Q(t)$ and let the interfacial heat flux from the well-mixed region to the diffusive region be $Q_i(t)$. Conservation of thermal energy shows that the uniform temperature of the well-mixed layer obeys

$$\dot{T}_m = \frac{Q - Q_i}{\rho C_p h}, \tag{3}$$

where ρC_p is the heat capacity of the fluid per unit volume and the dot denotes a derivative with respect to time. As a result of the continuity conditions at the interface,

$$\frac{Q_i}{\rho C_p} = \kappa \frac{\partial T_+}{\partial z}, \tag{4}$$

$$\dot{T}_m = \frac{\partial T_+}{\partial t} + \dot{h} \frac{\partial T_+}{\partial z}, \tag{5}$$

where the subscript + denotes a value just above the interface.

Equations (1)–(5) are straightforward, and equivalent equations are likely to feature in any simple model of penetrative convection at low Péclet number. However, the system is not as yet complete and can be regarded as missing either a boundary condition for the diffusion equation (1) or an equation for the interfacial velocity; equation (5) cannot serve both purposes. To see this more clearly, we combine (3)–(5) to obtain

$$h \frac{\partial T_+}{\partial t} + (h\dot{h} - \kappa) \frac{\partial T_+}{\partial z} = \frac{Q}{\rho C_p}. \tag{6}$$

Equation (6) is a mixed boundary condition for (1) if $\dot{h}$ is known, or an equation for $\dot{h}$ if the value of $\partial T_+/\partial z$ is known so that T_+ can be calculated from (1) and (2).

The physical idea that is required to close the problem is that of competition between the tendency of the interfacial heat flux to stratify the underlying fluid and the tendency of the convective eddies to erode the overlying stratification. For example, if the basal heat flux Q were suddenly set to zero then the convecting layer would restratify (albeit initially very weakly) in the short time taken for the convective eddies to come to rest, and h would become zero. Conversely, if Q were suddenly increased then we would expect to see a corresponding increase in $\dot{h}$. Considerations such as these suggest that the motion of the interface is related to the current value of Q and determined by the ability of convective eddies driven by the positive buoyancy flux at the base to mix the negative buoyancy flux across the interface through the depth of the well-mixed layer. Thus we write the remaining boundary condition as

$$Q_i = -kQ, \tag{7}$$

where k is a dimensionless entrainment coefficient.

A closure of similar form to (7) has been used in previous models of high-Péclet-number penetrative convection (e.g. Betts 1973; Carson 1973; Tennekes 1973), though in that context Q_i is given by $\dot{h}\Delta T$ rather than by (4), where ΔT is the interfacial discontinuity in temperature obtained by neglecting diffusion. (Extensions of (7) to grid-stirred mixing also replace Q by the turbulent kinetic energy flux near the interface.) Other models of entrainment at high Péclet number have been closed by expressing the dimensionless entrainment velocity $\dot{h}/u^*$ as a function of the interfacial Richardson number $Ri_i = \alpha g l^* \Delta T / u^{*2}$, where u^* and l^* are turbulent velocity and length scales. Many authors have observed that the two forms of closure are related and that an assumption that k is constant is equivalent to $\dot{h}/u^* \sim Ri_i^{-1}$. This

entrainment law has been supported by various theoretical and experimental studies of thermally stratified fluids but is known not to apply in all parameter regimes (see Turner 1973; Fernando 1991).

The value of k in the low-Péclet-number penetrative convection considered here may be expected to be determined by the vigour of the convection in the well-mixed layer. A convective velocity scale is given by $u^* = (\alpha g Q h/\rho C_p)^{1/3}$, where g is the gravitational acceleration and α is the coefficient of thermal expansion. The vigour of convection can thus be expressed by one of the following parameters: the convective Péclet number $Pe = u^* h/\kappa$; the flux Rayleigh number $Ra = Pe^3/Pr$; and the Reynolds number $Re = Pe/Pr$; where the Prandtl number is given by $Pr = \nu/\kappa$ and ν is the coefficient of kinematic viscosity. It follows that k can be expressed as a function of, say, Pe and Pr. However, the functional form of $k(Pe, Pr)$ is not yet known and in what follows we shall derive illustrative solutions under the simplest assumption that k is approximately constant. The good agreement with experimental results in §4 where the value of k was fixed by a one-point experimental measurement suggests that this approach is reasonable. If future experiments reveal the dependence of k on Pe and Pr then this could readily be incorporated into (7).

A little manipulation of (4) and (7) shows that the gradient Richardson number $Ri = \alpha g h^2(\partial T_+/\partial z)/u^{*2}$ is directly related to k by $Ri = kPe$ and hence we have not shown any dependence of k on Ri as would be customary in models of large-Péclet-number entrainment. This expresses the fact that the temperature gradient immediately above the interface, and hence the local Richardson number, are themselves determined by the competition between diffusive stratification and convective erosion. Thus the local Richardson number is a dependent rather than an independent parameter. The gradient Richardson number based on the original profile T_0 is not relevant since this only describes the temperature gradient a long way from the entrainment processes at the interface.

To show that (7) does indeed close the problem, we consider the equations in a frame translating at the speed of the interface. Equation (1) is written for $T(Z, t)$, where $Z = z - h(t)$, as

$$\frac{\partial T}{\partial t} = \dot{h}\frac{\partial T}{\partial Z} + \frac{\partial}{\partial Z}\left(\kappa\frac{\partial T}{\partial Z}\right). \tag{8}$$

From (3), (5) and (7)
$$\frac{\partial T}{\partial t} = \frac{Q(1+k)}{\rho C_p h} \quad \text{at} \quad Z = 0 \tag{9}$$

and from (4) and (6)
$$\frac{\partial T}{\partial Z} = \frac{kQ}{\rho C_p \kappa} \quad \text{at} \quad Z = 0. \tag{10}$$

We determine $\dot{h}$ by requiring that the solution of (8) subject to the boundary conditions (2) and (9) is compatible with the condition (10). For a given evolution of the interfacial temperature $T(Z = 0, t)$ and monotonically increasing far-field temperature $T_0(z)$, the solutions of (8) have the property that $\partial T(0, t)/\partial Z \to 0$ as $\dot{h} \to -\infty$ and $\partial T(0, t)/\partial Z \to \infty$ as $\dot{h} \to \infty$ (figure 2), thus enabling (10) to be satisfied by a suitable value of $\dot{h}$. Further consideration based on the solutions given in §3.1 shows that $\dot{h}$ is an increasing function of Q, that $\dot{h} \propto (t - t_0)^{-1/2}$ if Q undergoes a step change at $t = t_0$, and that h decreases suddenly to zero if Q is suddenly reduced to zero. Hence the boundary condition (7) makes both physical and mathematical sense.

It remains to comment on the solutions to equations equivalent to (1)–(5) presented by DW and Gubbins *et al.* (1982), which were derived without appeal to a boundary condition equivalent to (7). We have already noted that (1)–(5) are incomplete and

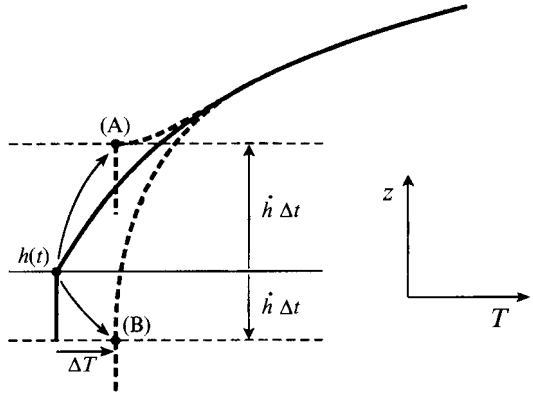

FIGURE 2. Suppose the temperature of the well-mixed layer increases by ΔT in time Δt. If the interface rises rapidly (A) then the temperature gradient above the interface is increased; if it descends rapidly (B) then the temperature gradient is decreased. There is a unique value of $\dot{h}$ which enables the flux boundary condition (7) to be satisfied.

cannot be solved without some form of closure. In the case of the solutions described above, this closure was provided implicitly, and perhaps unconsciously since no explanation was given, by the numerical algorithms used to solve the equations. For example, at each time-step DW fitted a simplified cubic equation to the temperatures at the last five grid points in the diffusion region, extrapolated the profile to obtain one 'ghost' point in the well-mixed region and then used this point to obtain a new interfacial temperature by explicit forward differencing. Thus the new interfacial temperature is specified as a function of the five old temperatures adjacent to the interface. This does give a boundary condition and a closed problem, but the physical meaning of this boundary condition is not clear.

3. Some simple solutions

Before comparing the theoretical model with experimental observations, we present solutions to two simple problems in order to illustrate some qualitative features of the model.

3.1. *Initially linear gradient with constant heat flux*

Consider an initially linear temperature gradient $T_0 = T_b + \Gamma z$ which is heated from below with a constant heat flux $Q = Q_0$ for $t > 0$. We choose an arbitrary vertical lengthscale L and define dimensionless variables by

$$\theta = \frac{T - T_b}{\Gamma L}, \quad \zeta = \frac{z}{L}, \quad \tau = \frac{\kappa t}{L^2}, \quad H = \frac{h}{L}, \quad \mathcal{Q} = \frac{Q}{\rho C_p \kappa \Gamma}. \tag{11a–e}$$

Equations (1)–(5) and (7) can then be rewritten as

$$\partial\theta/\partial\tau = \partial^2\theta/\partial\zeta^2, \tag{12}$$

$$\theta \to \zeta \quad \text{as} \quad \zeta \to \infty \quad \text{or} \quad \tau \to 0, \tag{13}$$

$$H\,\mathrm{d}\theta_+/\mathrm{d}\tau = (1+k)\,\mathcal{Q}, \tag{14}$$

$$\partial\theta_+/\partial\zeta = k\mathcal{Q}, \tag{15}$$

where, as before, the subscript + denotes the value immediately above the interface. The parameter $\mathcal{Q}$ is readily interpreted as the ratio of the applied heat flux to that conducted down the initial temperature gradient or, equivalently, as the global Péclet number.

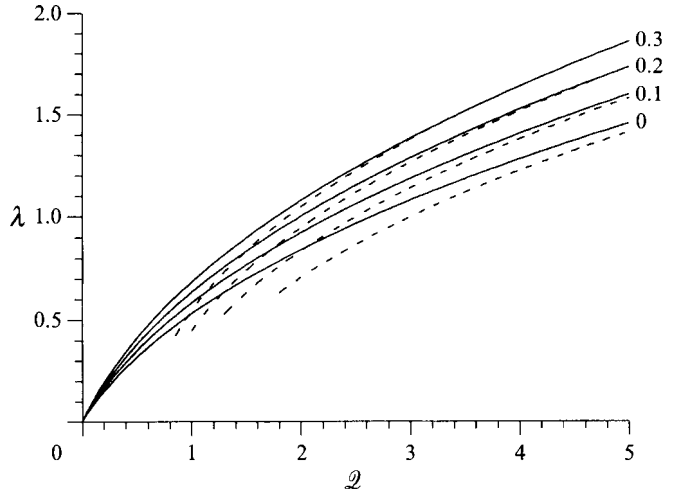

FIGURE 3. The solution $\lambda(\mathcal{2}, k)$ of (21) for $k = 0$, 0.1, 0.2 and 0.3 (solid lines). The asymptotic approximation (22) for $\mathcal{2} \gg 1$ is shown dashed. The dimensionless depth of the well-mixed region at the base of an initially linear temperature gradient heated uniformly from below increases according to $H = 2\lambda\tau^{1/2}$.

The independence of the scaled equations of the lengthscale L suggests that the solution of (12)–(15) is self-similar. We define a similarity variable

$$\eta = \zeta/(2\tau^{1/2}) \tag{16}$$

and seek a solution of the form

$$H = 2\lambda\tau^{1/2}, \quad \theta = 2\tau^{1/2} f(\eta). \tag{17}$$

Substitution into (12) and (13) shows that

$$f(\eta) = \eta + A \operatorname{ierfc} \eta, \tag{18}$$

where A is a constant and $\operatorname{ierfc} \eta$ is the first integral of the complementary error function $\operatorname{erfc} \eta$ (Abramowitz & Stegun 1965). The boundary conditions (14) and (15) imply

$$2\lambda f(\lambda) = (1+k)\,\mathcal{2}, \tag{19}$$

$$f'(\lambda) = k\mathcal{2}, \tag{20}$$

from which we obtain λ as the root of

$$2\lambda\left(\lambda + \frac{(1-k\mathcal{2})\operatorname{ierfc}\lambda}{\operatorname{erfc}\lambda}\right) = (1+k)\,\mathcal{2}. \tag{21}$$

Solutions for $\lambda(\mathcal{2}, k)$ are shown in figure 3 and some similarity temperature profiles $f(\eta)$ in figure 4. As would be expected, the rate of ascent of the interface increases with the heat flux $\mathcal{2}$ and with the entrainment coefficient k. The temperature gradient above the interface is greater than the initial gradient if $k\mathcal{2} > 1$.

As $\mathcal{2} \to \infty$

$$2\lambda^2 \sim \mathcal{2}(1+2k) - 1 \quad \text{and} \quad A \sim k\mathcal{2}/(2\lambda), \tag{22}$$

from which we can show that the perturbation temperature profile tends to a step of magnitude $\Delta\theta = k\mathcal{2}/\dot{H}$ in this limit. This establishes a formal link with models of high-Péclet-number penetrative convection though it should be emphasized that different mechanisms of entrainment are operative at high Péclet number and the present theoretical framework may not be appropriate.

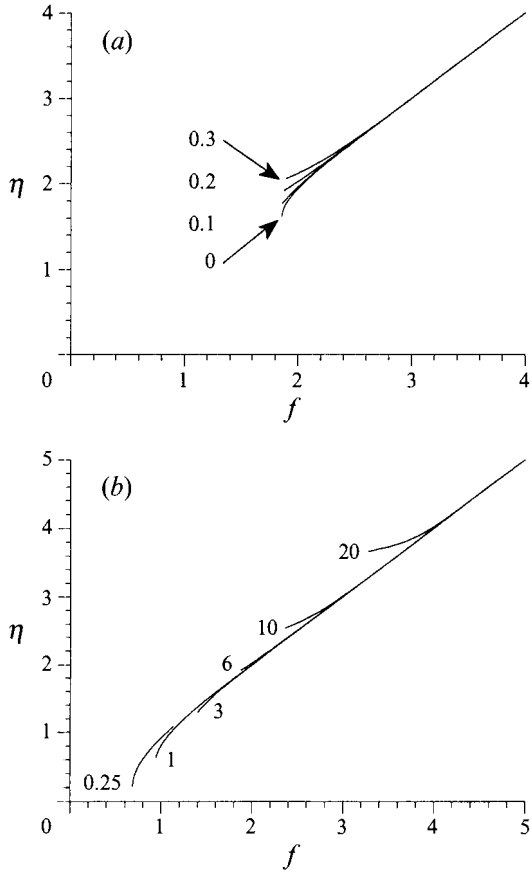

FIGURE 4. Self-similar temperature profiles $f(\eta)$ for an initially linear temperature gradient heated uniformly from below. The temperature below $\eta = \lambda$ (the end of the curves) is uniform. (*a*) $\mathcal{Q} = 6$ and $k = 0$, 0.1, 0.2 and 0.3; (*b*) $k = 0.2$ and $\mathcal{Q} = 0.25$, 1, 3, 6, 10 and 20.

The analysis may be taken a little further by considering the case in which the dimensionless heat flux is increased from $\mathcal{Q}$ to $\mathcal{Q}+\Delta\mathcal{Q}$ at time τ_0 with the interfacial height H_0 and temperature profile θ_0 given by (17). As a result of the increase in heat flux, the interfacial temperature gradient is increased by $k\Delta\mathcal{Q}$ and the rate of change of the interfacial temperature by the finite amount $(1+k)\Delta\mathcal{Q}/H_0$. We expect a temperature perturbation to diffuse away from the interface as the profile adjusts to the new heat flux and so we look for a local short-time solution of the form

$$H \sim H_0 + 2\Lambda(\tau-\tau_0)^{1/2}, \tag{23a}$$

$$\theta \sim \theta_0(\xi) + 2(\tau-\tau_0)^{1/2} g(\xi) \sim 2(\tau-\tau_0)^{1/2}\{k\mathcal{Q}\xi + g(\xi)\}, \tag{23b}$$

where $\xi = \frac{1}{2}(\zeta - H_0)/(\tau-\tau_0)^{1/2}$. From the new interfacial boundary conditions we find that

$$g(\Lambda) + k\mathcal{Q}\Lambda = 0 \quad \text{and} \quad g'(\Lambda) = k\Delta\mathcal{Q}, \tag{24}$$

from which Λ is given by

$$\frac{\Lambda \operatorname{erfc}\Lambda}{\operatorname{ierfc}\Lambda} = \frac{\Delta\mathcal{Q}}{\mathcal{Q}} \tag{25}$$

(figure 5*a*). It will be noted that if the heat flux is reduced ($\Delta\mathcal{Q} < 0$) then $\Lambda < 0$ and the interface starts to descend as part of the convecting zone restratifies – the reduced heat

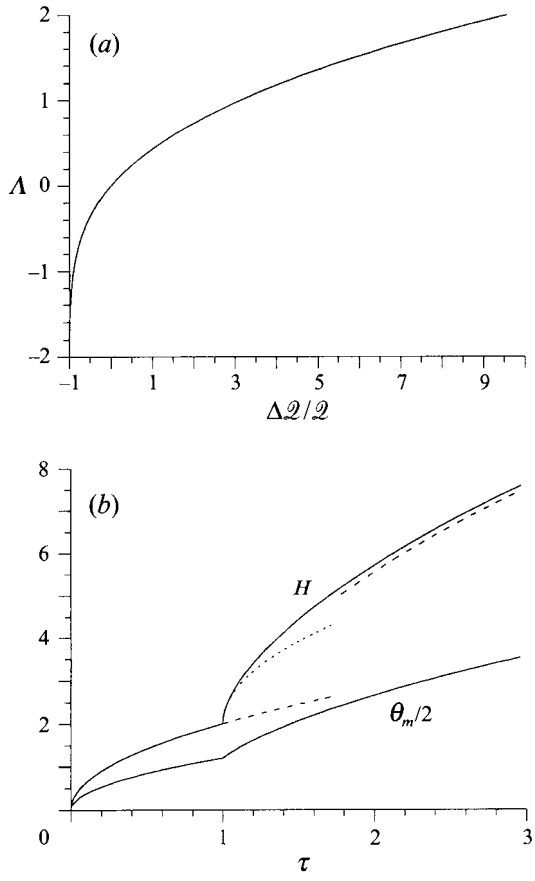

FIGURE 5. (*a*) The solution $\Lambda(\Delta\mathcal{Q}/\mathcal{Q})$ of (25) for the initial rate of interfacial rise after a step increase in the rate of basal heating from $\mathcal{Q}$ to $\mathcal{Q}+\Delta\mathcal{Q}$. If $\Delta\mathcal{Q} < 0$ then the interface starts to descend; if $\Delta\mathcal{Q}/\mathcal{Q} \to -1$ then $\Lambda \to -\infty$, corresponding to instantaneous restratification when the basal heat flux is removed. (*b*) The evolution of the interfacial height and mixed-layer temperature for $k = 0.2$ when the rate of heating is increased from $\mathcal{Q} = 2$ to $\mathcal{Q} = 10$ at $\tau = 1$. The numerical solution for H (solid curve) confirms the asymptotic solutions (17) (dashed curves) and (23) (dotted curve). The similarity solution at the new heating rate is evaluated at $\tau - 0.8$ in order to account for the period at the lower heat flux.

flux drives a weaker convective flow which is unable to carry the previous levels of negative buoyancy flux down from the interface. In the limit that the new heat flux $\mathcal{Q}+\Delta\mathcal{Q} \to 0$, the coefficient $\Lambda \to -\infty$, which suggests that the only solution in this case is instantaneous restratification of the entire convecting layer. While (23) describes the short-time behaviour after the change in heat flux, at large times the solution adjusts to the similarity form (17) for the new heat flux (figure 5*b*).

3.2. *Initially linear temperature with constant base temperature*

Consider now an initially linear temperature profile $T_0 = T_b + \Gamma z$ and suppose that the temperature at the base is suddenly changed at $t = 0$ to a fixed value T_B greater than T_b. After a very short transient the unstable boundary layer at the base will start to convect and a well-mixed convecting region will start to grow into the overlying gradient. The convection is driven by the heat flux due to the temperature difference between the interior of the well-mixed region and T_B. This temperature difference

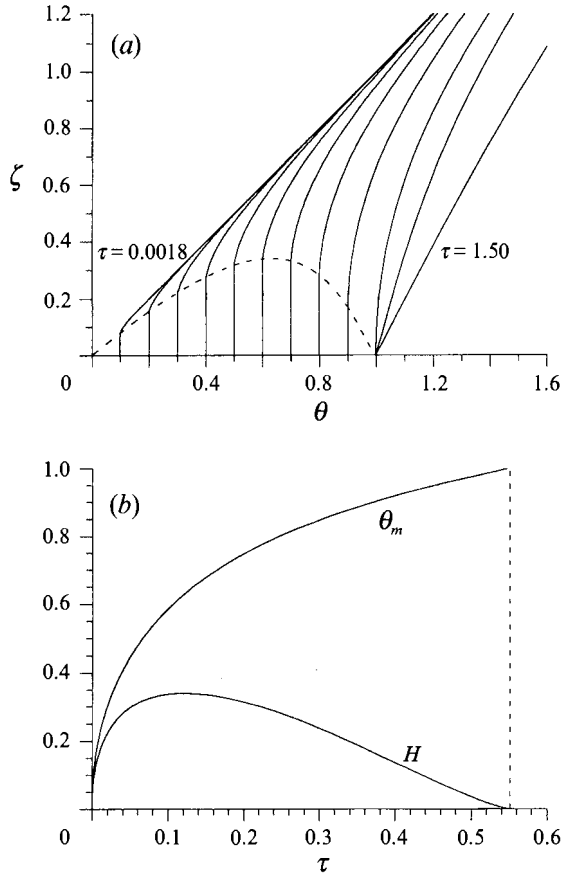

FIGURE 6. The evolution of an initially uniform temperature gradient heated from below at a rate $\mathcal{Q}(1-\theta_m)^{4/3}$, where $\mathcal{Q} = 2$. (*a*) Below the interface (dashed curve) the temperature is uniform and just above the interface the gradient is related to the current heat flux. As the mixed-layer temperature approaches unity, the heat flux decreases and the convecting zone restratifies. The temperature profiles $\theta(\zeta)$ correspond to times $\tau = 0.0018$, 0.0081, 0.020, 0.038, 0.066, 0.11, 0.16, 0.25, 0.37, 0.55, 0.75 and 1.50 (from left to right). (*b*) The variation of the mixed-layer temperature θ_m and interfacial height H with time τ. After $\tau \approx 0.551$ the convective zone vanishes and the subsequent evolution is by diffusion alone.

decreases as the mixed layer heats up and, as the convection weakens, the diffusive flux from above steadily restratifies the convecting layer until the thermal transport is once again by diffusion alone. We model this evolution by assuming that the heat flux driving convection depends on the temperature difference across the basal boundary layer by the usual four-thirds power law,

$$\frac{Q}{\kappa\rho C_p} = C\left(\frac{\alpha g}{\kappa\nu}\right)^{1/3}(T_B - T_m)^{4/3}, \tag{26}$$

where C is a constant and T_m is the interior temperature of the well-mixed layer (Turner 1973).

We follow the same non-dimensionalization as in (11) but with L chosen to be $(T_B - T_b)/\Gamma$. The resultant system of equations is again given by (12)–(15), but in which $\mathcal{Q}$ is no longer a constant. From (26) we find instead that

$$\mathcal{Q} = \mathcal{Q}_0(1-\theta_m)^{4/3}, \tag{27}$$

where $$\mathscr{Q}_0 = \frac{C}{\Gamma}\left(\frac{\alpha g}{\kappa\nu}\right)^{1/3}(T_B - T_b)^{4/3}. \tag{28}$$

The equations were solved numerically by mapping the diffusive region onto a fixed domain. At each time-step (12)–(14) were solved using a modified Crank–Nicholson method that was second-order in both space and time. The value of $\dot{H}$ was found iteratively using a root-finding algorithm so that (15) was satisfied at the conclusion of each time-step.

The solution of (12)–(15) and (27) is shown in figure 6 for the case $\mathscr{Q}_0 = 2$ and $k = 0.2$. At short times the solution is given by (17) and both H and θ_m increase rapidly. As the driving temperature difference $1-\theta_m$ decreases, the rate of interfacial rise also decreases (more rapidly than $t^{-1/2}$), and at $\tau = 0.12$, when $\theta_m = 0.63$ and H reaches a maximum value of 0.34, the convecting region starts to restratify. As $\theta_m \to 1$, the basal heat flux (27) and the depth of the convecting layer both decrease to zero, and at $\tau = 0.55$ convection ceases. The subsequent evolution is entirely diffusive and it is straightforward to show that the long-time behaviour is $\theta \sim \zeta + \operatorname{erfc}\eta$.

4. Comparison with experimental measurements

Having demonstrated that the theoretical model makes both mathematical and physical sense, it is clearly desirable to test the predictions of the model against experimental observations. An opportunity to do so is provided by the experiments described in DW on heating a stable temperature gradient from below. Three experiments were performed in a well-insulated Perspex tank, 30 cm by 30 cm in area and 60 cm in height. In each experiment the tank was filled to a total depth of 55 cm with a layer of hot water overlying a shallower layer of cold water. The experiments differ chiefly in the proportions of hot and cold water used to fill the tank (table 1). Though the filling process itself introduced some mixing and a broad gradient between the hot and cold layers, the experiments were left undisturbed for up to about an hour in order to allow the temperature gradient to develop throughout the lower part of the tank. At the end of this time a steady uniform heat flux $Q/\rho C_p = 0.023$ cm °C s^{-1} was then supplied electrically through the base of the tank. Further details can be found in DW. Thermocouples were used to determine both vertical temperature profiles at a given time and temporal temperature variations at a given height; the rise of the interface between the well-mixed and stratified regions was monitored visually.

In the calculations reported in DW, a small correction was made to account for the heat losses from the apparatus. In our calculations we model the heat losses very simply by using a Newtonian law of cooling at each height in the fluid column based on a surrounding temperature of 20 °C. Thus we add a small term of the form $-\sigma(T-20)$ to the right-hand sides of (1) and (3), where the decay constant σ is estimated to be about 3×10^{-6} s^{-1} from the reported experimental rate of decrease in the temperature T_a at the top of the tank (figures 7, 10 and 11 of DW) distant from the interfacial processes. Though Newtonian cooling is an approximation of the true heat losses, the term is small and of the right magnitude, and we do not expect the results to be significantly influenced by the details of the approximation.

From measurements of the vertical temperature profile DW estimated that at 170 min into experiment ES2 the ratio of the interfacial heat flux due to molecular diffusion to the basal heat flux was 0.13 (calculated as 77% of 0.17 from p. 15 of DW†).

† From measurements of the rate of change of the temperature profile DW suggested that the total interfacial heat flux may have been about 30% greater than the molecular value due to the effects of

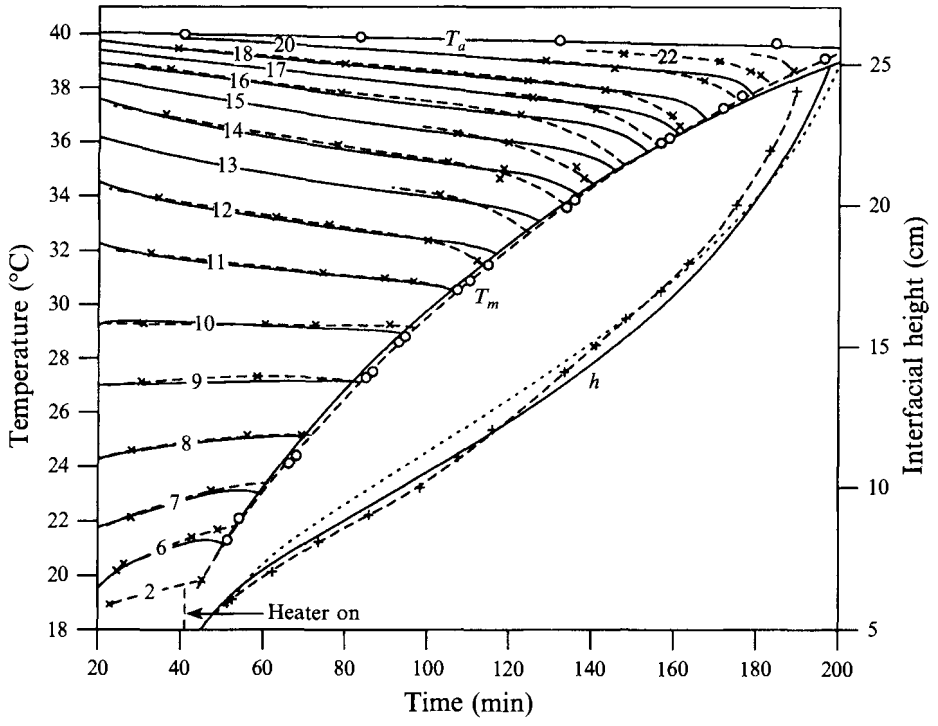

FIGURE 7. Calculated values (solid curves) of the temperature at various heights (labelled in cm), the interfacial and upper surface temperatures and the interfacial height for experiment ES1. The experimental measurements marked +, × and ○ and the fitted dashed curves are reproduced from figure 11 of DW. The dotted curve represents the numerical calculation of the interfacial height by DW.

Expt	d_g (cm)	T_{m0} (°C)	T_{a0} (°C)	t_h (min)
ES1	10.0	17.7	40.1	41
ES2	13.9	20.5	39.2	73
ES3	23.6	10.0	38.4	32.5

TABLE 1. Parameters for the experiments of DW. A depth d_g of fluid of temperature T_{m0} is initially overlain by fluid of temperature T_{a0} to a total depth of 55 cm. At time t_h heating of the lower boundary commences

Accordingly, in our calculations we use a constant value $k = 0.13$ for all three experiments and, as stated earlier, we also take the diffusivity κ to be constant and equal to the molecular value. We note that we had no reason *a priori* to expect k to be constant during and between experiments and the justification for our choice of a constant value lies in simplicity and in the good agreement obtained with the experimental observations. Noticeably worse agreement is obtained by use of the values $k = 0.12$ or $k = 0.14$.

Thus the calculations to be presented are based on the modified forms of equations (1) and (3), and (4), (5) and (7). The initial conditions are given by the reported

turbulent diffusion. However, given the experimental uncertainties in obtaining rates of change near an oscillating interface, it is not clear that this difference is significant and we choose to use the more directly calculated molecular value.

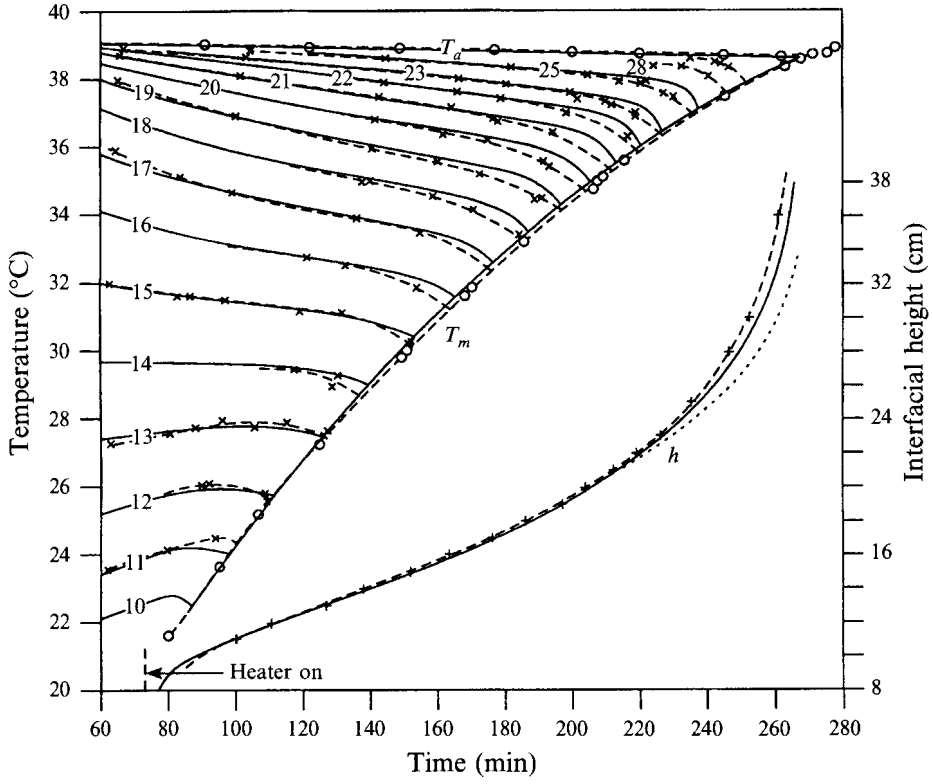

FIGURE 8. As figure 7 but for experiment ES2, with data from figure 7 of DW.

temperature profiles (figures 7, 10 and 11 of DW) at 20 min (ES1), 60 min (ES2) and 0 min (ES3), which are prior to the commencement of heating. A no-flux boundary condition is applied at the top of the fluid, $z = 55$ cm, since any experimental heat losses from the top have been included in the Newtonian cooling term. The equations are solved using a numerical scheme similar to that outlined in §3.2. It will be noted that the model as described, with Newtonian heat losses, constant coefficients and no wave-enhanced diffusion, is almost the simplest possible. Nevertheless, the calculations give excellent agreement with the experimental observations, which suggests that the model does encapsulate the dominant physical processes. Refinements of the model are possible but are not justified either by the quality of the data or by our present level of knowledge about the detailed mechanisms of turbulent entrainment.

In figures 7–9 we present the experimental observations of DW and our numerical predictions for the evolution of the interfacial height, the mixed-layer temperature and the temperatures at a number of fixed depths in the same style as figures 7, 9 and 11 of DW. The agreement between observation and prediction is, in general, at least comparable to that obtained by DW (using their unusual numerical boundary condition) and in some cases, notably experiment ES1, is significantly better. In all cases, the agreement with the measurements of the interfacial height is better.

The importance of diffusive heat transfer across the interface is shown by several qualitative features present in both the predictions and the observations. Firstly, fluid above the interface is cooled by heat transfer to the underlying well-mixed layer, causing the temperature at a given height to dip downward as the interface approaches. Secondly, the pre-cooling of fluid above the interface allows the interface to rise

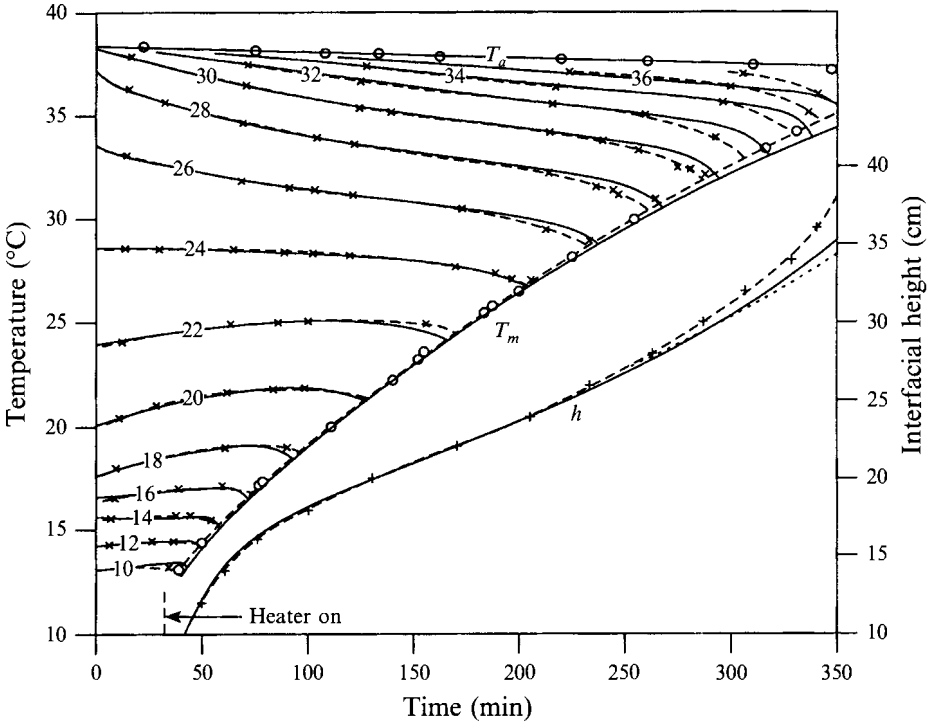

FIGURE 9. As figure 7 but for experiment ES3, with data from figure 10 of DW.

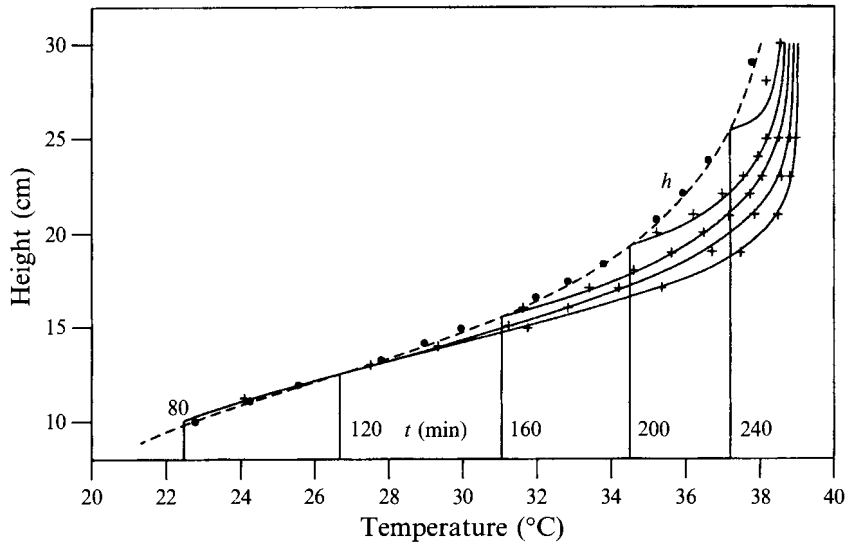

FIGURE 10. Calculated temperature profiles at various times and the interfacial temperature as a function of interfacial height for experiment ES2. Points marked + or ● are experimental measurements reproduced from figure 8 of DW.

significantly faster than if the interfacial heat flux were ignored (see figure 6 of DW). Thirdly, a plot of the vertical temperature profiles at a succession of times (figure 10) clearly shows the diffusive evolution of the stably stratified region on the timescale of the interfacial motion.

Towards the end of the experiments there is a tendency for the experimental observations to show a greater depth of cooled fluid above the interface than in the numerical predictions. By this stage the interface has risen through the region of strongest temperature gradient and is starting to advance rapidly into the relatively unstratified fluid at the top of the tank. We suggest that the greater cooling above the interface may be caused by large-amplitude wave motions at late times which enhance the effects of molecular diffusion in the weakly stratified region. At earlier times the good agreement with the model predictions suggests that the effects of wave motion are negligible unless the stratification is very weak.

5. Discussion

We have presented a simple two-layer model of penetrative convection at low Péclet number. A well-mixed layer is separated from a stably stratified layer by an interface across which both the temperature and the heat flux are continuous. The temperature of the well-mixed layer is calculated from a global heat budget based on the fluxes across its boundaries; the temperature of the stably stratified layer evolves according to the diffusion equation. The interfacial motion is determined by an entrainment assumption which expresses the heat flux across the interface as a fraction $k(Pe, Pr)$ of the heat flux driving convection.

This model may usefully be contrasted in a number of aspects with the sort of model usually employed to describe high-Péclet-number penetrative convection. In a high-Péclet-number model, the initial temperature profile is 'frozen' and does not diffuse on the timescale of the evolution of the well-mixed layer. As a result of the neglect of diffusive fluxes, the interface is capable of supporting a discontinuity in the temperature, which is generated by mechanical erosion of the initial profile by eddies impinging from below. The interfacial heat flux at high Péclet number is thus given by the erosion of the temperature discontinuity rather than by diffusion down the temperature gradient above the interface and the Richardson number is an independent rather than a dependent variable. The heat budget for the well-mixed layer and the closure on the interfacial motion by an entrainment assumption on the interfacial heat flux are, however, similar in the two cases. The chief difference between the present model and previous models of penetrative convection at low Péclet number is that the previous models were not closed by an entrainment equation.

The entrainment equation embodies the key physical concept that there is a competition between the tendency of the interfacial heat flux to restratify the underlying fluid and the tendency of the convective eddies to erode the overlying stratification. By consideration of what happens if the heat flux driving convection is greatly increased or reduced to zero, it is clear that it is this competition that determines the rate of interfacial motion. Whereas erosive deepening of the mixed layer is always dominant at high Péclet number, both growth of the mixed layer by erosive deepening and decay by restratification can occur at low Péclet number. Particular solutions to the model in which the depth of the well-mixed layer decreases by restratification have been demonstrated in two cases where the driving heat flux is decreasing.

Similarity solutions have been found for the cases of an initially uniform gradient heated at a constant rate and of the transient response to a sudden change in the rate of heating. A numerical scheme based on a shooting method for the interfacial flux condition has been described for more general problems. This scheme was used to reanalyse the experimental data of DW, showing it to be in very good agreement with the present model. This agreement is remarkable since the calculations were based on

a single fixed value of the entrainment parameter k, which might in principle depend on the convective Péclet number (or Rayleigh or Reynolds numbers) of the flow and hence vary between and during experiments. Though a fixed value of k corresponds to the well-known Ri^{-1} entrainment law in a high-Péclet-number context, that does not explain its occurrence in the present parameter regime. The value of k chosen, 0.13, was fixed by one experimental measurement and further experiments are clearly desirable to determine the (possibly weak) dependence of k on Pe and Pr. Such experiments need to be in the regime (see Appendices) in which convection is sufficiently vigorous to keep the convective layer well-mixed but not so vigorous that rising thermals penetrate a greater distance than the diffusion distance in the stable region. These conditions are favoured by large layer depths, relatively inviscid fluids and strong initial temperature gradients.

It would also be of interest to extend our investigations to low-Péclet-number situations in which the turbulence in the well-mixed layer is generated by grid-stirring or a mean shear flow rather than convection. In these cases, the spatial variation of the turbulent intensity must be taken into account, as in Hopfinger & Linden (1982), and the entrainment condition (7) would need to be modified accordingly. Comparison could then be made with the grid-stirred experiments of Noh & Fernando (1993) in which entrainment was diffusion dominated but the effects of diffusion were confined to the interfacial zone and did not affect the bulk of the unmixed region. From such extensions, it is to be expected that a further range of solutions that show an intriguing competition between erosion and restratification will result.

I am grateful to S. S. S. Cardoso, H. E. Huppert, R. C. Kerr, P. C. Matthews, J. S. Turner and M. G. Worster for thoughtful and constructive comments on an earlier version of this manuscript and to I. R. Wood for providing further information about the experiments described in DW.

Appendix A. The penetration distance of rising thermals

We present a simple scaling argument to determine the conditions under which the penetration distance of rising thermals into the stable region is less than the diffusive lengthscale, thus allowing us to neglect region IV of figure 1(*a*) in comparison with region I.

Let $\hat{T}'$ denote the typical magnitude of the temperature gradient in the stratified region. Hence the ratio of the advective flux in the convecting region to the typical conductive flux in the stable region (a global Péclet number) is given by

$$Pe_g \sim Q/(\rho C_p \kappa \hat{T}'). \tag{A 1}$$

The convective Péclet number (the ratio of convection to conduction in the convecting region) is given by

$$Pe_c \sim \hat{u}h/\kappa, \tag{A 2}$$

where $\hat{u}$ is the typical velocity scale for the rising thermals

$$\hat{u} \sim [\alpha g Q h/(\rho C_p)]^{1/3}. \tag{A 3}$$

A simple estimate of the penetration distance δ_p of rising thermals is given by balancing the typical kinetic energy of the thermal with the potential energy created by penetration into the stable overlying gradient (see e.g. Phillips 1977). Thus

$$\tfrac{1}{2}\rho\hat{u}^2 \sim \tfrac{1}{2}\rho\alpha\hat{T}' g\delta_p^2 \tag{A 4}$$

from which we obtain $$\delta_p/h \sim (Pe_g/Pe_c)^{1/2}. \tag{A 5}$$

The rate of rise of the interface $\dot{h}$ may be estimated from

$$\dot{T}_m \sim \dot{h}\hat{T}' \sim Q/(\rho C_p h) \tag{A 6}$$

and the diffusion distance δ_c ahead of the interface from

$$\delta_c \sim (\kappa h/\dot{h})^{1/2}. \tag{A 7}$$

Thus $$\delta_c/h \sim 1/Pe_g^{1/2}. \tag{A 8}$$

Hence the condition $\delta_p \ll \delta_c$ requires $Pe_c \gg Pe_g^2$. The condition that the convective layer is well-mixed further requires $Pe_c \gg 1$.

Consideration of the dependence of these conditions on Q suggests that the present model is appropriate for an intermediate range of basal heat flux. At very low rates of heating the convection is insufficiently vigorous to keep the convective layer well-mixed. At very high rates of heating the interface advances rapidly so that the penetration distance of thermals is greater than the diffusion distance in the stable layer. These constraints should be kept in mind for the design of future investigations into the functional dependence of the entrainment coefficient k. It should also be noted that the arguments above are based on a high-Reynolds-number inertia–buoyancy balance in which viscous forces are neglected. Modifications may thus be necessary for high-Prandtl-number fluids, in which convection can occur at high Rayleigh number but only moderate to low Reynolds number (Appendix B).

Appendix B. Convection at high Prandtl number

In this Appendix we discuss the application of our model to convection at high Prandtl number in which the dynamics are governed by a viscous–buoyancy balance and there is a significant separation between the scales of the viscous and thermal boundary layers. A useful comparison can be made with the results of experiments by Jaupart & Brandeis (1986), in which a layer of hot silicone oil was simultaneously cooled from top and bottom. A well-mixed convecting zone driven by cooling from above occupied most of the layer while a relatively thin stagnant zone formed at the base of the layer due to the cooling at the lower boundary. The Prandtl number ranged from 175 to 8850, the Rayleigh number from 10^6 to 10^8 and the typical Reynolds number was of order 0.1 (based on $\nu = 1$ cm^2 s^{-1}, a plume spacing of order 1 cm and a plume velocity of order 0.1 cm s^{-1}).

The experimental observations motivate a two-layer model of the form considered in this paper, in which the heat flux at the top is given by (26) and the boundary condition (2a) is replaced by a fixed-temperature boundary condition at the lower boundary. Jaupart & Brandeis (1986) set $Q_i = 0$ and $h = d$, the total depth of the layer, to obtain an approximate solution for T_m,

$$T_m = (1+t)^{-3}, \tag{B 1}$$

in suitable dimensionless variables. The diffusive evolution of the temperature in the stagnant layer was approximated by making the similarity ansatz that $T(z,t) = T_m(t)f\{z/[d-h(t)]\}$, where the shape function f satisfies $f(0) = 0$ and $f'(1) = 0$. The global heat balance for the stagnant layer then shows that

$$h^2 = \frac{3}{C\,Ra^{1/3}}\left(\frac{2f'(0)}{1+5F}\right)((1+t)-(1+t)^{-6F/(1-F)}), \tag{B 2}$$

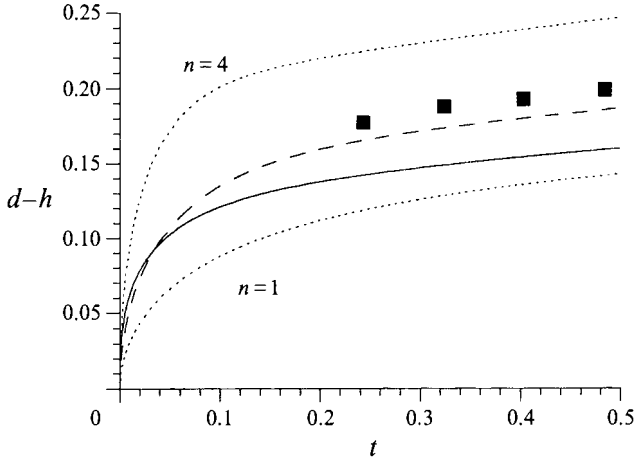

FIGURE 11. The dimensionless thickness $d-h$ of the stagnant zone in a layer of high-Prandtl-number fluid cooled from above and below at initial Rayleigh number 1.8×10^8. Approximate solutions based on Jaupart & Brandeis (1986) derived from a shape function $f = 1-(1-x)^n$ with $n = 2$ (dashed) and $n = 1$ or 4 (dotted). Solution of the present model (solid) and data from Jaupart & Brandeis (solid squares).

where $F = \int_0^1 f(x)\,\mathrm{d}x$ and Ra is the initial Rayleigh number. Reasonable agreement with the experimental data was obtained with $f = x(2-x)$ (figure 11) though, since the diffusion equation was not actually solved, this choice is somewhat arbitrary. Other choices, such as $f = 1-(1-x)^n$ with $n > 1$, agree less well.

Numerical solution of the full system of equations (i.e. (1)–(5), (7) and (26) suitably modified), also shows the dependence $h \propto Ra^{-1/6}$, which is confirmed experimentally. The depth of the stagnant layer, however, is underestimated by about 20% (figure 11), even for $k = 0$. This suggests that descending thermals, rather than entraining fluid from the top of the stagnant zone and mixing it through the convecting zone, are instead detraining, underplating the convecting zone and increasing the depth of the stagnant zone. Indeed, this behaviour is to be expected given the large Prandtl number and low Reynolds number of the flow. From a theoretical point of view, a boundary condition at the interface is still required to solve the diffusion equation (1). These considerations suggest that at large Prandtl number and low Reynolds number this condition should take the form of a detrainment condition based on a viscous–buoyancy balance rather than the entrainment condition (7) which is based on an inertia–buoyancy balance.

REFERENCES

ABRAMOWITZ, M. & STEGUN, I. A. 1965 *Handbook of Mathematical Functions*. Dover.

BETTS, A. K. 1973 Non-precipitating cumulus convection and its parameterization. *Q. J. R. Met. Soc.* **99**, 178–196.

CARMACK, E. C. & FARMER, D. M. 1982 Cooling processes in deep temperate lakes: A review with examples from two lakes in British Columbia. *J. Mar. Res.* **40**, 85–111.

CARSON, D. J. 1973 The development of a dry inversion-capped convectively unstable boundary layer. *Q. J. R. Met. Soc.* **99**, 450–467.

CRAPPER, P. F. & LINDEN, P. F. 1974 The structure of turbulent density interfaces. *J. Fluid Mech.* **65**, 45–63.

DEARDORFF, J. W., WILLIS, G. E. & LILLY, D. K. 1969 Laboratory investigation of non-steady penetrative convection. *J. Fluid Mech.* **35**, 7–31.

DEARDORFF, J. W., WILLIS, G. E. & STOCKTON, B. H. 1980 Laboratory studies of the entrainment zone of a convectively mixed layer. *J. Fluid Mech.* **100**, 41–64.

DENTON, R. A. & WOOD, I. R. 1981 Penetrative convection at low Péclet number. *J. Fluid Mech.* **113**, 1–21 (referred to herein as DW).

FERNANDO, H. J. S. 1991 Turbulent mixing in stratified fluids. *Ann. Rev. Fluid Mech.* **23**, 455–493.

FERNANDO, H. J. S. & LITTLE, L. J. 1990 Molecular-diffusive effects in penetrative convection. *Phys. Fluids* A **2**, 1592–1596.

FERNANDO, H. J. S. & LONG, R. R. 1985 On the nature of the entrainment interface of a two-layer fluid subjected to zero-mean-shear turbulence. *J. Fluid Mech.* **151**, 21–53.

GUBBINS, D., THOMSON, C. J. & WHALER, K. A. 1982 Stable regions in the Earth's liquid core. *Geophys. J. R. Astron. Soc.* **68**, 241–251.

HANNOUN, I. A. & LIST, E. J. 1988 Turbulent mixing at a shear-free density interface. *J. Fluid Mech.* **189**, 211–234.

HOPFINGER, E. J. & LINDEN, P. F. 1982 Formation of thermoclines in zero-mean-shear turbulence subjected to a stabilizing buoyancy flux. *J. Fluid Mech.* **114**, 157–173.

HOWARD, L. N. 1966 Convection at high Rayleigh number. In *Proc. 11th Intl. Congr. Appl. Mech., Munich,* pp. 1109–1115. Springer.

JAUPART, C. & BRANDEIS, G. 1986 The stagnant bottom layer of convecting magma chambers. *Earth Planet. Sci. Lett.* **80**, 183–199.

KERR, R. C. 1991 Erosion of a stable density gradient by sedimentation-driven convection. *Nature* **353**, 423–425.

LICK, W. 1965 The instability of a fluid layer with time-dependent heating. *J. Fluid Mech.* **21**, 565–576.

LINDEN, P. F. 1973 The interaction of vortex rings with a sharp density interface: a model of turbulent entrainment. *J. Fluid Mech.* **60**, 467–480.

MORY, M. 1991 A model of turbulent mixing across a density interface including the effect of rotation. *J. Fluid Mech.* **223**, 193–207.

NOH, Y. & FERNANDO, H. J. S. 1993 The role of molecular diffusion in the deepening of the mixed layer. *Dyn. Atmos. Oceans* **17**, 187–215.

PHILLIPS, O. M. 1977 *The Dynamics of the Upper Ocean.* Cambridge University Press.

ROUSE, H. & DODU, J. 1955 Turbulent diffusion across a density discontinuity. *Houille Blanche* **10**, 522–532.

SCHWARZSCHILD, M. 1958 *Structure and Evolution of Stars.* Princeton University Press.

TENNEKES, H. 1973 A model for the dynamics of the inversion above a convective boundary layer. *J. Atmos. Sci.* **30**, 558–567.

TURNER, J. S. 1973 *Buoyancy Effects in Fluids.* Cambridge University Press.

ZILITINKEVICH, S. S. 1991 *Turbulent Penetrative Convection.* Avebury.